Journal of Engineering Science and Technology
Vol. 12, No. 7 (2017) 1723 - 1739
© School of Engineering, Taylor's University

DEVELOPMENT OF AN INTELLIGENT PRESSURE SENSOR WITH TEMPERATURE COMPENSATION

VAEGAE NAVEEN KUMAR[1],
KOMANAPALLI VENKATA LAKSHMI NARAYANA[2,*]

[1]School of Electronics Engineering, VIT University, Vellore
[2]School of Electrical Engineering, VIT University, Vellore, Tamil Nadu, India - 632014
[*]Corresponding Author: kvlnarayana@vit.ac.in

Abstract

This paper presents the design of an artificial neural network (ANN) based intelligent pressure sensor to measure pressure in the range 0-100 psig with high accuracy and temperature compensation. A capacitive pressure sensor detects the applied pressure by means of elastic deflection of diaphragm. A Modified Schering Bridge Signal Conditioning Circuit (MSB-SCC) converts the change in capacitance of the sensor into an equivalent voltage. The effect of change in environmental conditions, especially effect of ambient temperature on the pressure sensor and component drifts, stray effects associated with MSB-SCC introduce nonlinearity and cross-sensitivity errors in the output readout. The ANN trained with Levenberg-Marquardt (LM) algorithm incorporates the intelligence into sensor signal conditioning circuit through a microcontroller unit to reduce the nonlinearity effects and compensate the cross-sensitivity errors.The LM algorithm shows better performance in terms of the linearity error in comparison with Broyden-Fletcher-Goldfarb-Shanno (BFGS) and the Scaled Conjugate Gradient (SCG) algorithms. The proposed method is experimentally verified at various temperatures and it provides voltage readout within ±0.8% of full-scale reading over a range of temperature variations from 10°C to 35°C.

Keywords: Artificial neural network, Diaphragm, Modified Schering bridge circuit, Multilayer perceptron, Pressure measurement, Temperature compensation.

1. Introduction

Pressure is one of the most important physical quantities to be measured, monitored and controlled in any process industry. The operating principle of pressure sensor is based on the conversion of a result of pressure exertion on a

Nomenclatures

b	Bias of artificial neuron
C,C_o,C_1,C_3,C_4	Capacitance , nF
$C(P)$	Capacitance as a function of pressure
$C(P,T_A)$	Capacitance as a function of pressure and temperature
E	Modulus of elasticity, psig
FSR	Full scale reading
h	Hidden neuron output
I	Input to neuron
MV	Measured value, V
NF	Normalization factor
O	Output of final layer neuron
P	Pressure, psi
R	Diaphragm radius, mm
R_1, R_2, R_3	Resistance, Ω
S	Weighted sum of artificial neuron
T_o, T_A	Temperature, °C
t_m	Diaphragm thickness, mm
TV	True value, V
V	Weighted inputs of artificial neuron
$V_{ac},V_{dc},V_o,V_P,V_s,$ V_A,V_{ANN1},V_{ANN2}	Voltage, V
W	Weights of artificial neuron
W_o	Deflection of the diaphragm, mm
Z_1,Z_2,Z_3,Z_4	Impedance, Ω

Greek Symbols

ω	Frequency, rad./sec.
E	Error in percentage
ν	Poisson's ratio,
θ_1,θ_2	Constants of capacitance – temperature approximation

Abbreviations

ANN	Artificial Neural Network
BFGS	Broyden-Fletcher-Goldfarb-Shanno
LM	Levenberg-Marquardt
MLP	Multilayer Perceptron
MSB	Modified Schering Bridge
PIM	Plug in Module
RISC	Reduced Instruction Set Computer
SCC	Signal Conditioning Circuit
SCG	Scaled Conjugate Gradient

sensitive element into an electrical signal. Typically, exertion of pressure results in the displacement or deformation of an element having a defined surface area and thus, pressure measurement may be reduced to a measurement of a displacement or force. Variable capacitive transducers are mostly used to convert the displacement changes into an electrical signal. A suitable signal conditioning circuit is to be designed to measure the small changes in capacitance corresponding to the changes in pressure for the capacitive transducer.

In literature, various capacitance measurement methods have been proposed by different investigators to accurately measure the small change in capacitance. Takagi and Yamakawa [1] proposed a simple and wide-range capacitance measuring equipment using transistor blocking oscillator. It has a limitation in that the unknown capacitor cannot be tested at a desired frequency and voltage. Analog signal conditioning circuits with passive components for measurement of capacitance are presented with electrical readout [2, 3]. A microprocessor-based switched battery capacitance meter reported in [4] is simple, but the measured values do not reflect the accepted equivalent circuit parameters applicable to sinusoidal excitation. A simple method for the measurement of capacitance and dissipation factor of capacitor proposed in [5] has low resolution making it unsuitable for low value capacitance measurement. The conventional bridge methods measure capacitance with reliable electrical output, but these methods are tedious and time consuming, as convergence towards balance requires several iterative steps [6, 7]. Bera, Mandal and Sarkar [8] proposed a pressure sensor using improved inductance bridge circuit. The major drawback of the circuit is that the direct connection of inductance in the feedback path of operational amplifier provides derivative action to the input signal, which may damage the op-amp. Narayana and Bhujangarao [9] developed a pressure transmitter using modified inductance measuring network and bellow sensor, but the linearity of the method is ±2.5%.

The signal conditioning circuits in the reported methods measures pressure with reasonable results of accuracy and linearity, but these methods are proposed without considering the effect of ambient temperature. The ambient temperature introduces cross-sensitivity errors in the output readout. An effective signal conditioning circuit also suffers from stray effects, component tolerances and ageing etc. Hence the measurement scheme with the integration of intelligent capabilities through soft computing techniques presents a potential solution for minimizing and eliminating the nonlinearities. ANN based linearization methods have been proposed for various sensors [10-12]. An intelligent pressure transmitter has been proposed with computer simulations [11]. Kumar *et al*. [12] developed an ANN-based linearization method for a thermistor circuit. Even though the reported methods are suitable for pressure measurement, no methods reported so far to provide efficient solution for reduction of errors due to nonlinearities and cross-sensitivity effects. This motivates us to design and develop an efficient pressure sensor with intelligent capabilities to provide linearization and compensation functions.

In the present paper, the change in the capacitance of the pressure sensor due to applied pressure is converted into voltage using a MSB circuit. The MSB-SCC exhibits nonlinear relation between pressure and output voltage. ANN is used to estimate and compensate the nonlinearity of MSB-SCC along with temperature compensation. A microcontroller based plug-in-module (PIM) is proposed to implement the ANN technique. The design aspects, simulation analysis and experimental results of the proposed method are reported. The effectiveness of the method has been experimentally verified.

2. Proposed Method

The proposed pressure sensor with linearization and compensation procedures is depicted in Fig. 1. In the linearization procedure, MSB-SCC produces an

analog- voltage proportional to the change in capacitance of the sensor due to the applied pressure. The MSB-SCC generates a stable readable output proportional to the measured pressure and reduces the high non-linearity error of the capacitive pressure sensor to an extent. The relation between the input pressure and MSB- SCC voltage is quite nonlinear. ANN-1 estimates and reduces the nonlinearity of MSB-SCC.

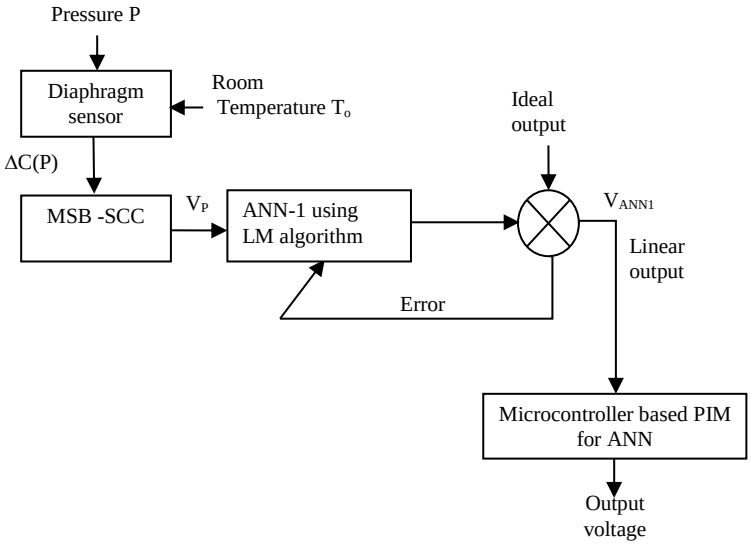

(a) Linearization.

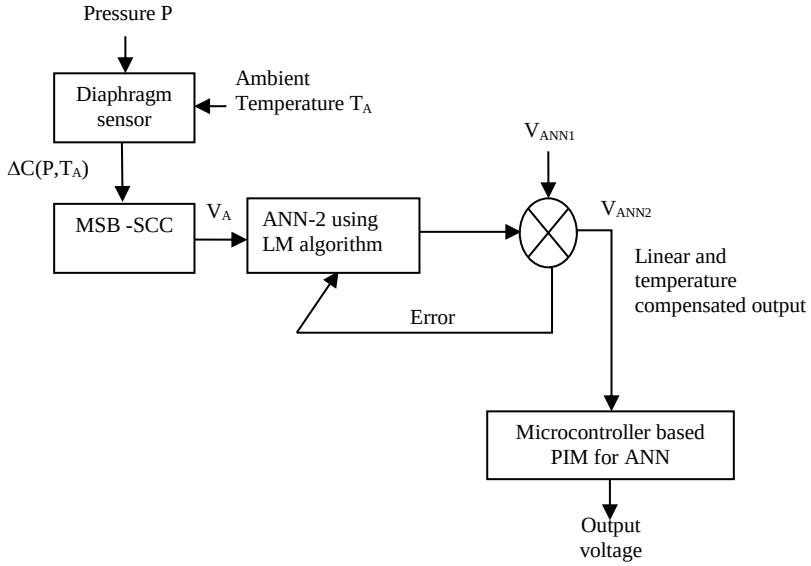

(b) Compensation.

Fig. 1. Block diagram of the proposed intelligent pressure sensor.

In the compensation procedure, MSB-SCC produces an analog voltage proportional to the change in capacitance due to applied pressure and ambient temperature. The ambient temperature introduces cross-sensitivity errors in the output readout and is compensated by ANN-2. In both the procedures, the Multi-Layer Perceptron (MLP) neural network implementing Levenberg-Marquardt (LM) algorithm estimates the non-linear characteristic of the MSB-SCC and the intelligence of the ANNs is embedded in a PIM for practical implementation. The following sections describe the design and functional aspects of various stages of the proposed method.

2.1. Design of sensor signal conditioning circuit

The capacitive pressure sensor and associated signal conditioning circuit is shown in Fig. 2. The capacitive pressure sensor detects the applied pressure by means of the elastic deflection of the diaphragm. The relation between deflection of the diaphragm and applied pressure [13] is

$$P = \left(\frac{16Et_m^4}{3R^4(1-\nu^2)} \right) \left(\frac{W_o}{t_m} + 0.488 \left(\frac{W_o}{t_m} \right)^2 \right) \tag{1}$$

where P is the applied pressure, W_o is the deflection of the diaphragm, E is modulus of elasticity, t_m is diaphragm thickness, ν is Poisson's ratio, R is diaphragm radius to clamped edge. For a typical diaphragm structure, the deflection is proportional to applied pressure, P and the capacitance, $C_1(P)$ is approximated by [14]

$$C_1(P) = C_o + \Delta C_1(P) \tag{2}$$

where C_o is the offset capacitance at zero pressure and $\Delta C_1(P)$ is the change in capacitance. Also, the sensor capacitance changes with ambient temperature, T_A and is expressed as

$$C_1(P, T_A) = C_o f_1(T_A) + \Delta C_1(P, T_o) f_2(T_A) \tag{3}$$

where $\Delta C_1(P, T_o)$ is the change in capacitance due to applied pressure at reference temperature T_o. The functions $f_1(T_A)$ and $f_2(T_A)$ are given by

$$f_1(T_A) = 1 + \theta_1(T_A - T_o) \tag{4}$$

$$f_2(T_A) = 1 + \theta_2(T_A - T_o) \tag{5}$$

Here θ_1, θ_2 are constants, $f_1(T_A)$ and $f_2(T_A)$ are obtained at three different ambient temperatures 10°C, 15°C and 35°C. The capacitance values at different temperatures for different pressures can be found by substituting these values in Eq. (3). The diaphragm capacitive sensor forms one arm of the MSB and produces a change in its capacitance due to applied pressure. The MSB-SCC consists of modified Schering bridge, differential amplifier, rectifier and voltage follower circuit. The MSB produces an ac output voltage, V_{ac} proportional to change in capacitance of the arm 1.

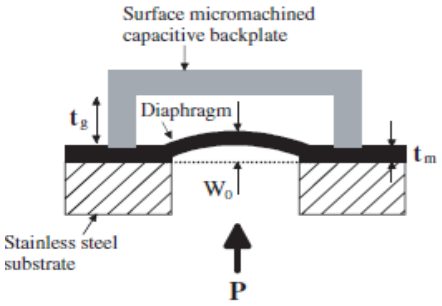

(a) Capacitive pressure sensor.

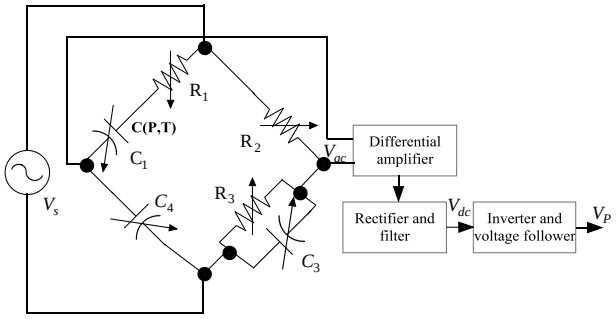

(b) MSB-SCC.

Fig. 2. Pressure sensor and associated signal conditioning circuit.

The MSB output voltage is further amplified, converted into dc voltage and inverted as output voltage V_o. Under balanced condition

$$Z_1 Z_3 = Z_2 Z_4 \tag{6}$$

$$\left(R_1 + \frac{1}{j\omega C_1}\right)\left(\frac{R_3}{1+ j\omega C_3 R_3}\right) = \left(\frac{R_2}{j\omega C_4}\right) \tag{7}$$

Separating imaginary and real parts equating and, we get

$$R_1 = \left(\frac{R_2 C_3}{C_4}\right) \tag{8}$$

$$C_1 = \frac{C_4 R_3}{R_2} \tag{9}$$

The output voltage of MSB under measurement or unbalanced condition is

$$V_{ac} = \left(\frac{j\omega C_4\left(1+ j\omega R_1 C_1(P,T_A)\right)}{j\omega C_1(P,T_A)\left(1+ j\omega R_1 C_4\right)+ j\omega C_4} - \frac{R_2\left(1+ j\omega R_3 C_3\right)}{R_2\left(1+ j\omega R_3 C_3\right)+ R_3}\right) V_s \tag{10}$$

2.2. ANN modeling technique

The ANN based modeling of MSB-SCC for linearization and compensation is shown in Figs. 3 and 4 respectively. ANN-1 and ANN-2 comprise of a simple MLP neural network with one input, one hidden and one output layer. The MLP architecture consisting of only three layers is an efficient solution for sensor linearization [15] as it is simple in implementation and requires reduced number of operations. The nonlinear operation of MLP-ANN compensates the nonlinear characteristic of MSB-SCC. The input and output layers of ANN-1 and ANN-2 consist of one neuron each, whereas five neurons are present in hidden layer of ANN-1 and three neurons in hidden layer of ANN-2. In both the schemes, the hidden layers use tan hyperbolic function and output layers use linear function as activation functions. The nonlinearity of tan hyperbolic activation function is smooth and differentiable everywhere [16]. The training and learning process for ANN-1 and ANN-2 is implemented by LM-algorithm. The important features of LM algorithm are faster convergence time and lowest mean square error [17], [18]. The LM algorithm combines the features of steepest descent method and Gauss–Newton algorithm and is the most efficient algorithm for training small and medium sized problems [19], [20].

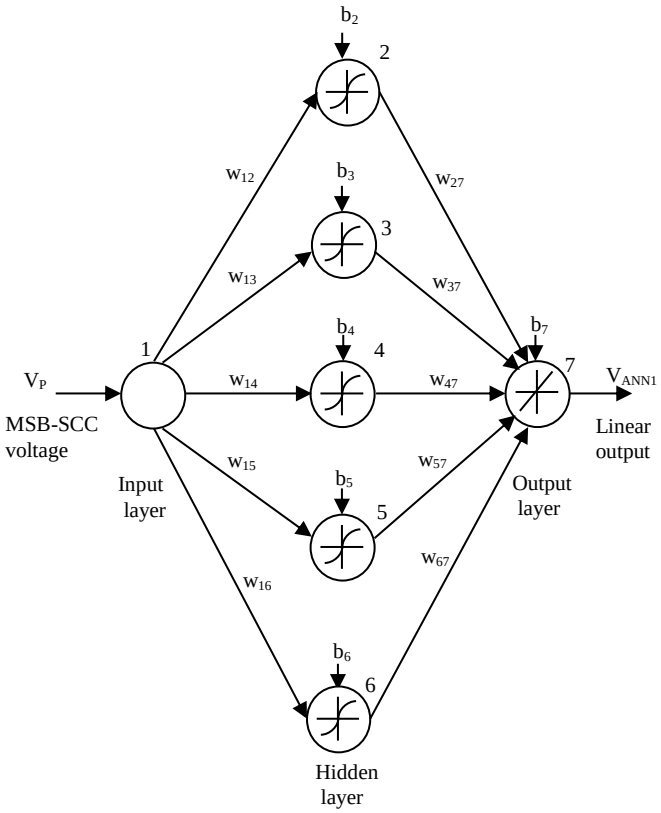

Fig. 3. ANN-1 scheme for linearization.

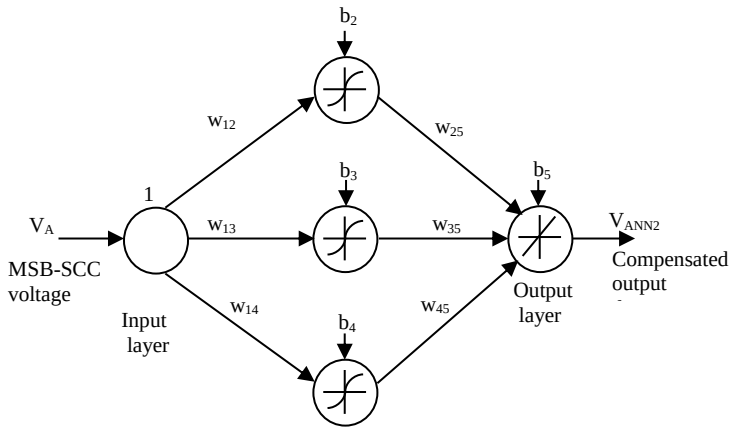

Fig. 4. ANN-2 scheme for compensation.

In ANN-1 scheme, the output voltage of MSB-SCC is applied as input to MLP and the target data for MLP is a straight line with unit slope. In ANN-2 scheme, the output voltage of MSB-SCC at ambient temperatures 10°C, 15°C and 35°C is applied as input to MLP and the output of ANN-1 is the target data. The LM algorithm trains the MLPs and iteratively updates the weights and biases. The coding for the MLPs is carried out in MATLAB. The output of ANN-1 and ANN-2 schemes is the linearized voltage V_{ANN1} and the compensated voltage V_{ANN2} respectively. The plug in modules for ANN-1 and ANN-2 schemes is shown in Figs. 5 and 6 respectively. The PIMs embeds the intelligence of ANN by performing necessary operations on the frozen weights and biases through registers, multipliers and adders. The registers of PIMs store weights, biases, weighted inputs, intermediate sum, activation functions and output of ANN schemes. In the PIMs, *W*, *b*, *V*, *h*, represents weights, biases, weighted inputs, and hidden layer outputs respectively, whereas *S* and *O* represents weighted sum and output of final layers.

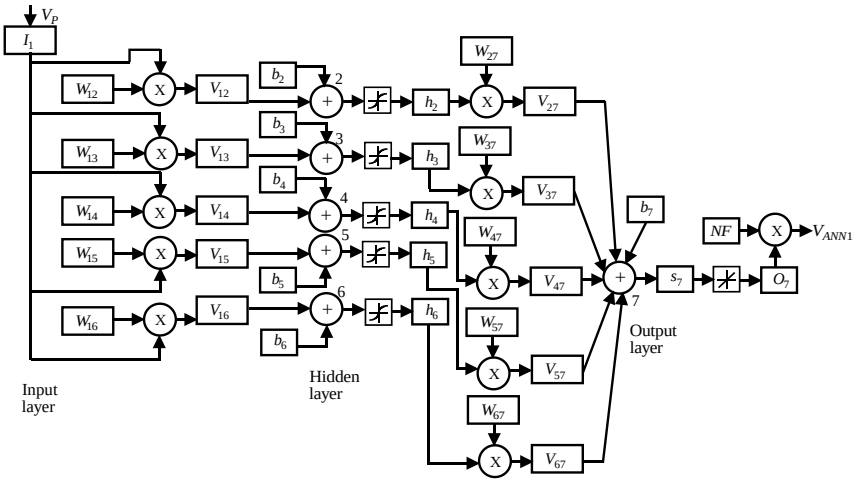

Fig. 5. Plug in module of ANN-1 for linearization.

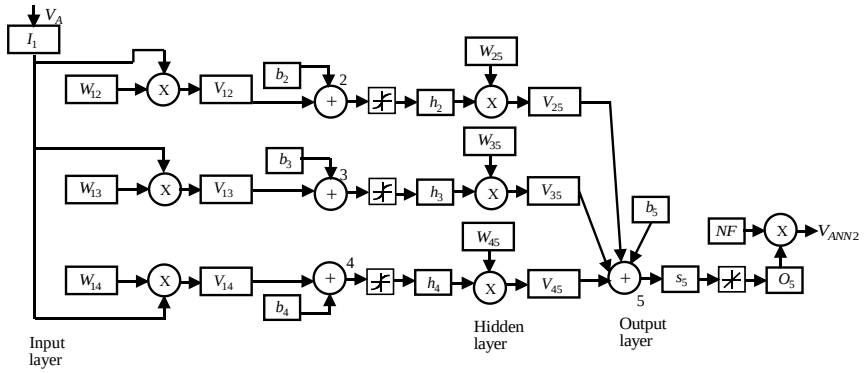

Fig. 6. Plug in module of ANN-2 for compensation.

Also *NF* denotes normalization factor to be multiplied with the output of ANN to get the physical linearized voltage. A micro-controller embedded unit is used to implement PIM.

3. Results and Discussion

The experimental set-up of the proposed scheme is shown in Fig. 7. The diaphragm is subjected to a pressure supplied from a pressure tank which is fitted with a gauge to measure gauge pressure. The deflection of the diaphragm produces a change in capacitance of the sensor and is measured by a LCR meter. An air conditioning mechanism is used to maintain the environment temperature at various values and the change in capacitance of diaphragm capacitive sensor at different temperatures is measured. The room temperature for linearization is 27°C and ambient temperatures considered are 10°C, 15°C and 35°C for compensation. The pressure versus change in capacitance of the diaphragm at temperatures 10°C, 15°C, 27°C and 35°C is plotted and shown in Fig. 8. The graph clearly illustrates the effect of ambient temperature on the sensor operation. The MSB-SCC converts capacitance change into dc voltage. The op-amps of MSB-SCC are OP 07 operational amplifiers as they provide high input impedance and ultra low-offset voltage. The output voltages of MSB-SCC for different values of the air pressure and temperatures are measured in both increasing and decreasing modes by three-and-one-half digit voltmeter.

The nonlinear MSB-SCC output voltage is applied as input to ANN-1 for linearizing scheme. In the training phase, 15 data points are chosen from the experimental data of MSB-SCC output voltage in the pressure range 0-100psig. The target data for the ANN-1 is a straight line with unit slope. During testing phase, the data points which are not used in training phase are applied as inputs to ANN-1. The outputs of the ANN-1 in the testing phase are closely matched to the desired response. After training, all the information of the linearization remains embedded in only ten weight values and six bias values. The linearized output V_{ANN1} is the target for the ANN-2 for compensating scheme. The MSB-SCC output voltage at temperatures 10°C, 15°C and 35°C is applied as inputs to ANN-2. In the training phase, 15 data points are chosen from the experimental data of the MSB-SCC output voltage in the pressure range 0-100psig. After training, all the information of

compensation remains embedded in only six weight values and four bias values. The parameters of ANN-1 and ANN-2 are presented in the Table 1.

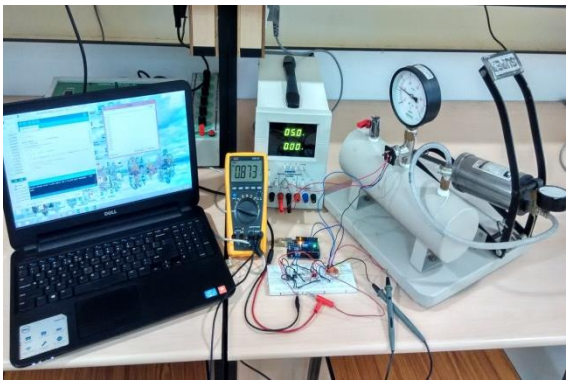

Fig. 7. Experimental setup of intelligent pressure sensor.

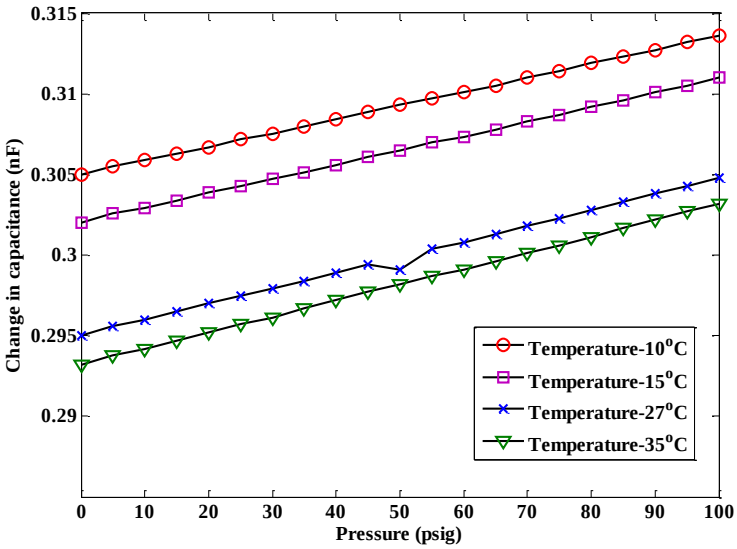

Fig. 8. Pressure versus capacitance characteristic of the diaphragm sensor.

The plug in modules for ANN-1 and ANN-2 is implemented by ATmega328 microcontroller unit which is operated at a maximum frequency of 20 MHz and coding has been done in AVR studio. ATmega328 is a high performance, low powered, low cost microcontroller with enhanced RISC architecture features.The nonlinearity error is obtained for the MSB-SCC and ANN schemes and the percentage nonlinearity error is obtained as,

$$\varepsilon = \frac{MV - TV}{FSR} \times 100 \tag{11}$$

where ε is the percentage nonlinearity error, *MV* is the measured value, *TV* is the true value and *FSR* is the full scale reading.

Figures 9 and 10 shows output voltage versus pressure characteristic and error analysis of the MSB-SCC and ANN schemes respectively for linearization. The compensated output voltage versus pressure characteristic and error analysis of the MSB-SCC and ANN schemes are shown in Figs. 11 and 12 respectively. The effectiveness of the ANN scheme is clearly reflected from the graphs as its output closely matches the desired response. The error analysis of the LM-ANN scheme is presented in Table 2 along with BFGS and SCG ANN schemes. It is observed that the LM-ANN scheme exhibits low linearity error in comparison to BFGS and SCG ANN schemes.

Table 1. ANN Training parameters and simulation results.

Neural network	Multilayer feed-forward neural network			
Activation function	Tan hyperbolic for hidden layer, Linear activation function for output layer			
Training algorithm	Levenberg-Marquardt			
Temperature	10°C	15°C	27°C	35°C
Number of hidden neurons	3	3	5	3
Epochs	61	25	14	50
Weights	W_{12}=1.15 W_{13}=1.05 W_{14}=-6.25 W_{25}=1.83 W_{35}=0.89 W_{45}=-0.13	W_{12}=-4.19 W_{13}=-1.35 W_{14}=-1.90 W_{25}=-0.08 W_{35}=-0.76 W_{45}=-0.55	W_{12}=-7.06 W_{13}=6.07 W_{14}=-6.76 W_{15}=-7.54 W_{16}=-9.60 W_{27}=-0.16 W_{37}=0.23 W_{47}=-0.19 W_{57}=-0.27 W_{67}=-0.21	W_{12}=-3.88 W_{13}=0.79 W_{14}=-3.18 W_{25}=-0.53 W_{35}=1.28 W_{45}=-0.16
Biases	b_2=-2.29 b_3=-0.06 b_4=-4.12 b_5=1.68	b_2=4.20 b_3=0.44 b_4=-1.71 b_5=-0.09	b_2=6.89 b_3=-3.52 b_4=1.04 b_5=-2.82 b_6=-7.73	b_2=5.24 b_3=-0.14 b_4=-2.59 b_5=0.56

Table 2. Error analysis of MSB-SCC and ANN schemes.

Scheme	**Temper-ature (°C)**	**Linearity error (%)**			
		MSB-SCC	**SCG**	**BFGS**	**LM**
Linearizing	**27**	**±3.0**	**±1.8**	**±1.7**	**±0.5**
Compensating	**10**	**±8.0**	**±4.0**	**±2.3**	**±0.8**
	15	**±2.0**	**±1.7**	**±1.3**	**±0.7**
	35	**±3.0**	**±2.0**	**±1.8**	**±0.8**

The comparative study of various signal conditioning methods for pressure measurement is presented in Table 3. The performance of the proposed intelligent pressure sensor is found to be quite linear with high degree of cross-sensitivity error compensation. The nonlinearity is specified as maximum deviation from the desired response. It has been observed that the nonlinearity of the linearization procedure lies within ±0.5% and nonlinearity of the compensation procedure lies within ±0.8%.

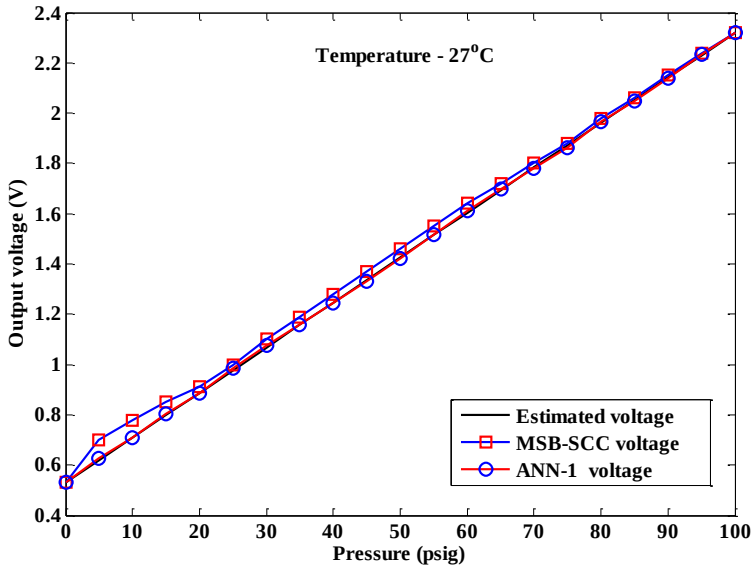

Fig. 9. Voltage-pressure characteristic.

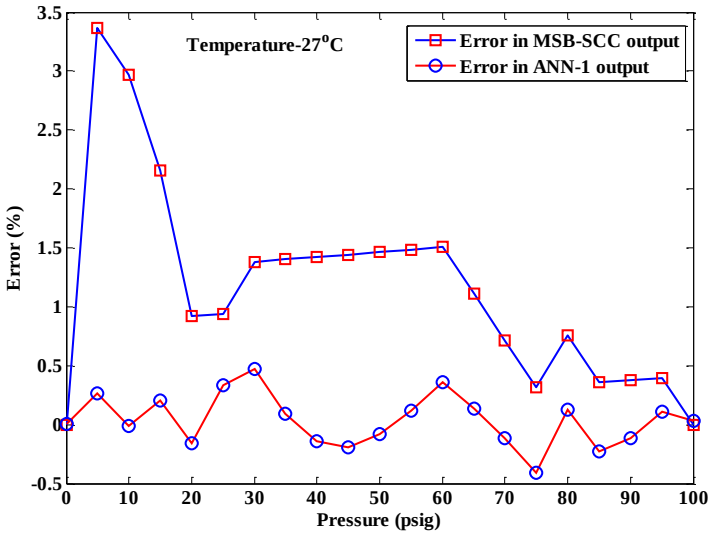

Fig. 10. Error analysis.

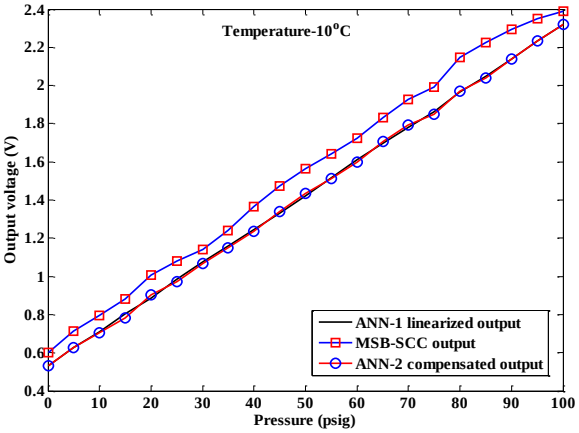

(a) Ambient temperature-10°C.

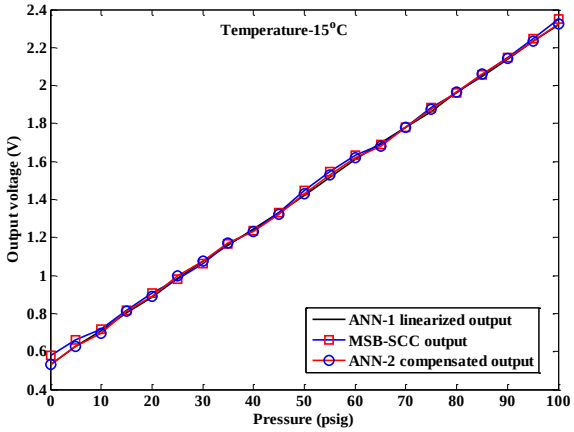

(b) Ambient temperature-15°C.

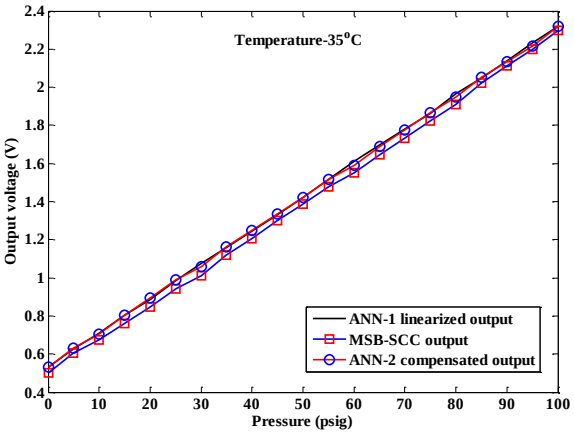

(c) Ambient temperature-35°C.

Fig. 11. Compensated output voltage versus pressure characteristic for MSB-SCC and ANN-2 schemes.

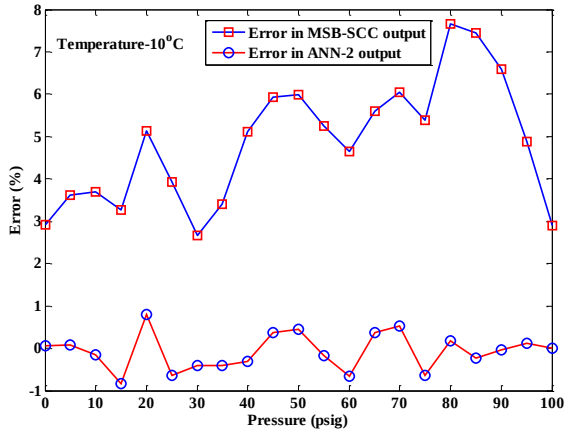

(a) Ambient temperature-10°C.

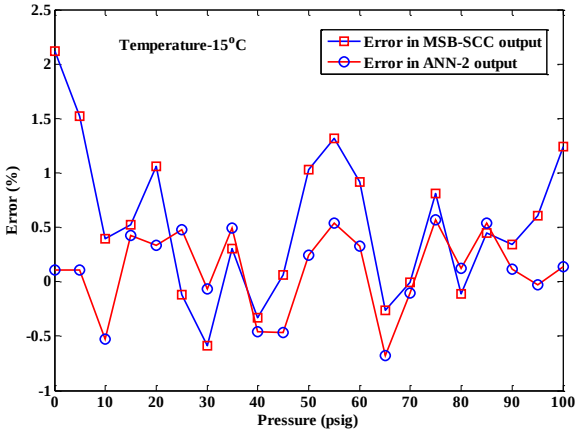

(b) Ambient temperature-15°C.

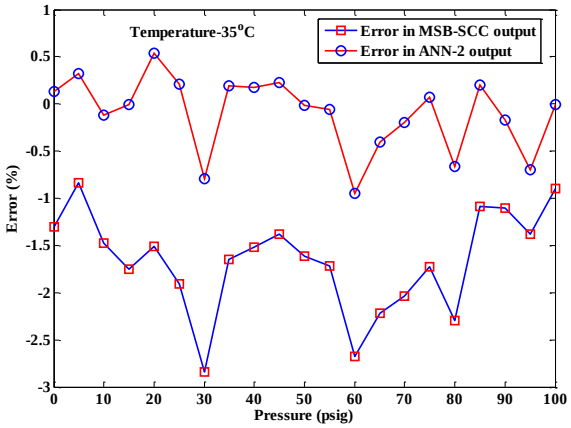

(c) Ambient temperature-35°C.

Fig. 12. Error versus pressure characteristic of MSB-SCC and ANN-2 schemes.

Table 3. Comparative study of various pressure measuring methods.

Technique	Range (psig)	Linearity	Notable feature
Improved inductance bridge circuit [8]. Bera et al. (2011)	0-45	±2%,	Time consuming, as convergence toward balance requires several iterative steps.
Intelligent pressure sensor [11]. Patra et al. (2011)	0-60	±1%	Suitable for wireless sensor applications.
Modified op-amp based network [9]. Narayana et al. (2013)	0-70	±3%,	Reduces errors due to stray capacitances, magnetic effects, but linearity is low.
ANN based pressure sensor. The authors.	0-100	10°C - ±0.8% 15°C - ±0.7% 27°C - ±0.5% 35°C - ±0.8%	Improved linearity with temperature compensation capability.

The notable feature of the method is temperature compensation throughout measuring range of pressure. The MLP-ANN with LM algorithm effectively overcomes the problems due to stray effects, balancing limitations, ambient conditions and component tolerances present in conventional and modified bridge circuits. The proposed method of pressure measurement posses improved characteristics comparable to the conventional methods available in literature.

4. Conclusions

An intelligent pressure sensing method using LM-ANN based signal conditioning circuit has been implemented with temperature compensation. The proposed method has been tested over the range of 0-100 psig with high linearity and accuracy. It effectively overcomes the limitations of passive circuits, conventional bridge, modified bridge and improved op-amp circuits. The plug in module of LM-ANN incorporates intelligence into signal conditioning circuit to make it free from component tolerances, environmental drifts and cross-sensitivity errors etc. The ANN-based linearizing and compensating scheme may be applied to various other sensors and transducers to nullify the adverse effects on their performance.

References

1. Takagi, T.; and Yamakawa, A. (1976). A simple and wide-range capacitance measuring equipment using transistor blocking oscillator. *IEEE Transactions on Instrumentation and Measurements*, 25(2), 162-163.

2. Thoma, P.E.; Stewart, R.; and Colla, J.O. (1980). A low pressure capacitance type pressure to electric transducing element. *IEEE Transactions on Components, Hybrids and Manufacturing Technology*, 3(2), 261-265.
3. Ansari, M.S.; and Ahmed, M.T. (1989). A novel direct reading active-RC system for measurements of in-circuit, discrete, and incremental capacitances. *IEEE Transactions on Instrumentation and Measurements*, 38(4), 922-925.
4. Mahmud, S.M.; and Rusek, A. (1988). A microprocessor-based switched battery capacitance meter. *IEEE Transactions on Instrumentation and Measurements*, 37(2), 191-194.
5. Jagadeesh Kumar, V.; Sankaran, P.; and Sudhakar Rao, K. (2003). Measurement of C and tanδ of a capacitor employing PSDs and Dual-slope DVMs. *IEEE Transactions on Instrumentation and Measurements*, 52(5), 1588-1592.
6. Holmberg, P. (1995). Automatic balancing of linear AC bridge circuits for capacitive sensor elements. *IEEE Transactions on Instrumentation and Measurements*, 44(3), 803-805.
7. Cutkosky, R.D. (1985). An automatic high-precision audio frequency capacitance bridge. *IEEE Transactions on Instrumentation and Measurements*, 34(3), 383-389.
8. Bera, S.C.; Mandal, N.; and Sarkar, R. (2011). Study of a pressure transmitter using an improved inductance bridge network and Bourdon tube as transducer. *IEEE Transactions on Instrumentation and Measurements*, 60(4), 1453-1460.
9. Narayana, K.V.L.; and Bhujangarao. A. (2013). Design and development of a pressure transmitter using modified inductance measuring network and bellow sensor. *Sensors & Transducers Journal*, 150(3), 32–39.
10. Medrano-Marques, N.J.; and Martin-del-Brio, B. (2001). Sensor linearization with neural networks. *IEEE Transactions on Industrial Electronics*, 48(6), 1288-1290.
11. Patra, J.C.; Meher, P.K.; and Chakraborty, G. (2011). Development of Laguerre neural network based intelligent sensors for wireless sensor networks. *IEEE Transactions on Instrumentation and Measurements*, 60(3), 725-734.
12. Kumar, V.N.; Narayana, K.V.L.; Bhujangarao, A.; and Sankar, S. (2015). Development of an ANN-based linearization technique for the VCO thermistor circuit. *IEEE Sensors Journal*, 15(2), 886-894.
13. Doeblin, E.O.; and Manik, D.N. (2004). *Measurements systems, fifth edition*. McGraw-Hill, New York, USA.
14. Yamada, M.; Watanabe, K. (1997). A capacitive pressure sensor interface using oversampling Δ-Σ demodulation techniques. *IEEE Transactions on Instrumentation and Measurements*, 46(1), 3-7.
15. Zhang, L.; and Tian, F. (2014). Performance Study of Multilayer Perceptrons in a Low-Cost Electronic Nose. *IEEE Transactions on Instrumentation and Measurements*, 63(7), 1670-1679.
16. Haykin, S. (1998). *Neural networks: A comprehensive foundation, second edition*. Prentice Hall, New Jersey, USA.

17. Levenberg, K. (1944). A method for the solution of certain problems in least squares. The *Quarterly of Applied Mathematics*, 2(2), 164-168.
18. Marquardt, D. (1963). An algorithm for least-squares estimation of nonlinear parameters. *SIAM Journal on Applied Mathematics*, 11(2), 431-441.
19. Wu, J.M. (2008). Multilayer Potts perceptrons with Levenberg-Marquardt learning. *IEEE Transactions on Neural Networks*, 19(12), 2032–2043.
20. Hagan, M.T.; Demuth, H.B.; Beale, M. (1996). *Neural Network Design*. Boston, MA, USA: PWS-Kent.